Interpretation of dilatometer tests in a heavy oil reservoir

Christophe Dano, Pierre-Yves Hicher, Damien Rangeard, Philippe Marchina

Interpretation of dilatometer tests in a heavy oil reservoir

Christophe Dano[1], Pierre-Yves Hicher[1], Damien Rangeard[2] and Philippe Marchina[3]

[1] *Research Institute in Civil and Mechanical Engineering, Ecole Centrale Nantes – University of Nantes – CNRS, 1 rue de la Noë, BP 92101, 44321 Nantes cedex 3, France*
[2] *Laboratoire de Génie Civil et Génie Mécanique, Institut National des Sciences Appliquées de Rennes, 20 avenue des Buttes de Coësmes, 35043 Rennes cedex, France*
[3] *Total E&P, Centre Scientifique et Technique Jean Feger, avenue Larribau, 64018 Pau, France*

This paper presents a prospective study for identifying selected parameters of the modified Cam-Clay model representing the behaviour of heavy oil reservoirs. The first part shows that the plastic compressibility, which controls the main recovery mechanism of such reservoirs, can be accurately determined, simultaneously with other parameters, by an inverse analysis of pressure–strain curves. The conditions of the identification procedure mainly involve two tests conducted under different drainage conditions or at different strain rates. The numerical study also establishes the sequence of an original *in situ* experimental program, in which three dilatometer tests at a relatively great depth (several hundreds of metres) were carried out. The comparison of the experimental data with the numerical computations reveals a significant over-consolidation ratio which does not allow the plastic compressibility to be determined but supports the findings regarding the geological erosion of the site.

KEY WORDS: dilatometer; identification; compressibility; petroleum

INTRODUCTION

In order to supply for the world's energy needs, oil companies are involved in expensive prospecting programs. In looking for lower costs, priority is given to prediction for evaluating the quality and the potential of oil fields, in particular the recoverable oil volumes. Geophysical

surveys thus aim at pinpointing potential hydrocarbon accumulations. Seismic imaging techniques and structural geology aim at assessing the on-site volumes, the over-pressured zones prior to drilling. However, the recoverable reserves need to be re-evaluated during production, since oil extraction induces compaction, which is a potentially important recovery mechanism for weakly cemented heavy oil reservoirs [1]. The magnitude of the compaction process depends mainly on the compressibility of the sand reservoir, which is not easily determined. Indeed, due to the very nature of this class of reservoirs, laboratory measurements may not always be reliable since the specimens are greatly disturbed during the coring process. To avoid this obstacle, it is preferable to carry out *in situ* compressibility measurements. The use of a dilatometer allowing the pressure–displacement characteristics of the formation to be determined has thus been considered.

DETERMINATION OF THE COMPRESSIBILITY FROM PRESSUREMETER TESTS

The feasibility of identifying the compressibility from a dilatometer test, whose principle is very close to the pressuremeter test used in geotechnical investigation, is closely examined in this first section. The tool used in the experimental program was designed on the basis of the dilatometer used in rock mechanics, different from the flat or plane dilatometer used for geotechnical investigations. The principle of the rock dilatometer, close to the one of the geotechnical pressuremeter, is subsequently described. Note that the word 'dilatometer' rather than 'pressuremeter' is used in the next sections, in reference to the rock mechanics device.

The compressibility considered here is the plastic compressibility λ, which is the slope of the virgin consolidation line in the $[v - \ln(p')]$ diagram where $v = 1 + e$ is the specific volume, e the void ratio and p' the mean effective stress. λ is one of the parameters of the modified Cam-Clay model [2] used in this study to model the mechanical behaviour of oil reservoirs. The modified Cam-Clay model is also characterized by the slope of the critical state line M in the $(p–q)$ diagram, the effective pre-consolidation pressure p'_{c0} and the initial void ratio e_0. The elastic behaviour implemented in the numerical code used for this study is considered linear and isotropic, characterized by the elastic modulus E and the Poisson's ratio v. The shear modulus is deduced by the relation $G = E/(2(1 + v))$. The elastic part of the model is different from the one usually found in the original Cam-Clay model characterized by the elastic compressibility κ. Therefore, in the following sections, the compressibility is defined by the compressibility factor β, which corresponds to the difference between the plastic compressibility λ and the elastic compressibility κ : $\beta = \lambda - \kappa$.

Choice of the modified Cam-Clay model

The Cam-Clay model might be seen as not very relevant for modelling the mechanical behaviour of a sand formation. Two points guided our choice. The first one lies in the fact that sandy soils, when subjected to high confining stresses, behave in a similar way as normally consolidated clayey soils. They can be highly contractant under deviatoric stresses and their decrease in void ratio during isotropic or one-dimensional consolidation shows a similar trend as the one obtained on clays: after a gentle slope up to a threshold point, the slope increases significantly and a linear relationship is observed in the $e - \log p'$ or $e - \log \sigma'_v$ plane, as for normally consolidated clays. The slope values remain smaller than the ones for clays, but can be

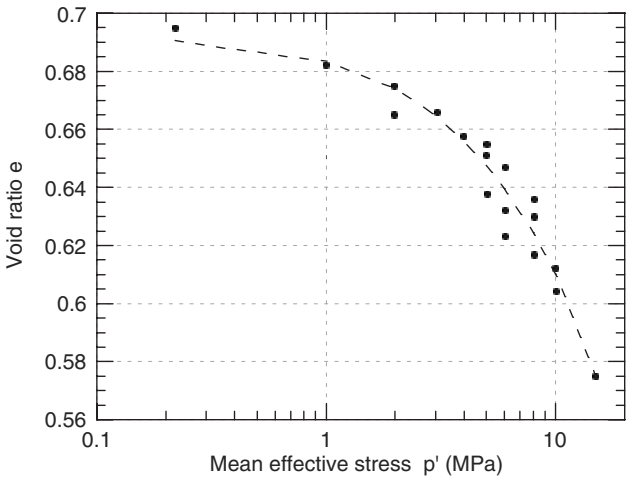

Figure 1. Isotropic test on Hostun sand (after Colliat-Dangus [4]).

considered in the same range of values as for low plasticity clays [3]. Figures 1 and 2 present some examples on Hostun sand subjected to isotropic and drained triaxial tests at high confining pressures [4]. These results show very similar behaviours as those observed on normally consolidated or slightly overconsolidated remolded clays. In particular, the critical state parameters can be deduced from the test results at large strains in a similar way as for clay.

The second point concerns previous works done on the interpretation of pressuremeter tests for determining the Cam-Clay parameters [5, 6]. A methodology was developed for identifying simultaneously mechanical Cam-Clay parameters and permeability from pressuremeter tests with strain holding stages. This procedure was successfully applied in the case of natural clay. Our purpose here is to rely on these previous studies for extending the methodology in the case of a sand reservoir.

Pressuremeter test results in clays

Rangeard *et al.* [6] showed that the compressibility factor β does not affect the pressure–volume curve in clayey soils for which the value of β is greater than 0.2, both in drained or undrained conditions. Therefore, the identification of the compressibility by inverse analysis becomes impossible since a large range of compressibility factors leads to the same pressure–volume curve. Zentar *et al.* [5], then Rangeard *et al.* [6] suggested methods to identify simultaneously two or three other parameters of the modified Cam-Clay model in clays. For instance, Zentar *et al.* [5] succeeded in determining the couples (G, M) or (G, p'_{c0}) from one pressuremeter curve obtained in undrained conditions and in determining the couple (M, p'_{c0}) from one pressuremeter curve in drained conditions. The simultaneous identification of the three parameters (G, M, p'_{c0}) requires additional information as for instance, the evolution of the pore water pressure Δu at the wall of the borehole [6].

It is also worth noting that because of the non-homogeneous stress field around the borehole, the loading at the cavity wall induces a partial drainage which depends on the loading rate and/or

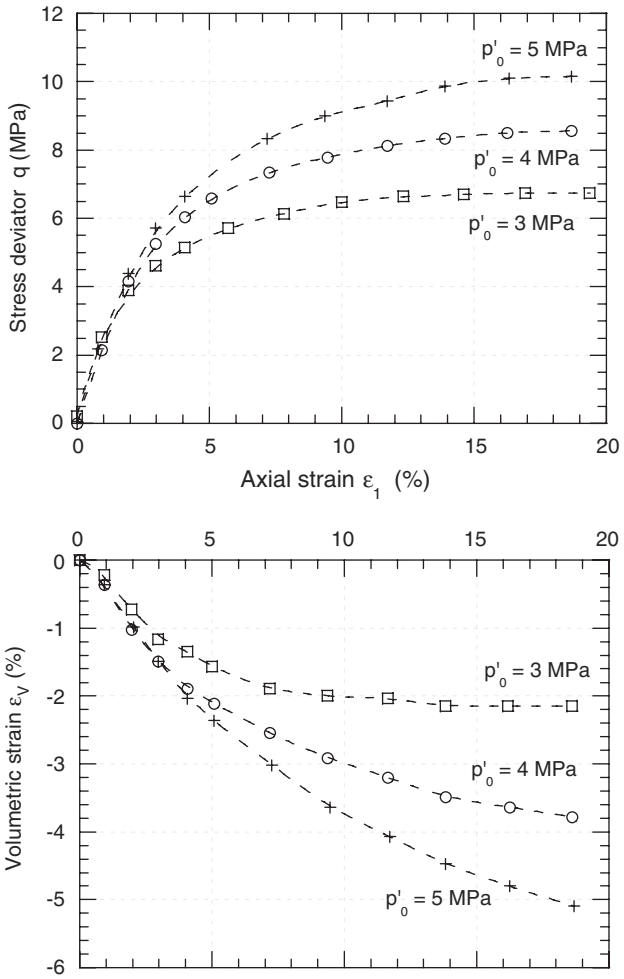

Figure 2. Triaxial tests on Hostun sand (after Colliat Dangus [4]).

the permeability of the tested soil. Rangeard *et al.* [7] put forward that the drainage state depends on a dimensionless coefficient D_k:

$$D_k = \frac{\partial \varepsilon_{a0}}{\partial t} \frac{a}{k} \tag{1}$$

where a is the initial radius of the cavity, k the permeability coefficient and $\partial \varepsilon_{a0}/\partial t$ the initial strain rate of the test. The main conclusions are the following [7]:

- the fully drained condition is obtained for high permeability coefficients and low strain rates: the value of D_k has to be lower than 10^{-2};
- the fully undrained condition is obtained for low permeability coefficients and high strain rates: the value of D_k has to be greater than 10^2;

Table I. Modified Cam-Clay parameters for sensitivity study.

Parameter	G	M	p'_{c0}	σ'_{r0}	σ'_{v0}	β
Unit	MPa		kPa	kPa	kPa	
	30.8	1.2	280	150	300	$0.02 \rightarrow 0.12$

Note: G shear modulus; M, slope of the critical state line; p'_{c0}, effective pre-consolidation pressure; σ'_{r0}, initial effective radial stress at the cavity wall; σ'_{v0}, initial effective vertical stress; β, compressibility factor.

- an intermediate behaviour characterized by the effect of the drainage on the total stress and the pore pressure evolutions at a degree more or less important depending on the value of D_k. A detailed description of that intermediate behaviour can be found in [7].

The previous observations also show that a constant value of the ratio $k/(\Delta\sigma_r(a)/\Delta t)$ where $\Delta\sigma_r(a)$ is the radial stress increment applied at the cavity wall during the time increment Δt leads to the same pressuremeter curve. It is therefore equivalent to study either the effect of the stress rate $(\Delta\sigma_r(a)/\Delta t)$ or the effect of the permeability k on the pressuremeter curve provided that the ratio $k/(\Delta\sigma_r(a)/\Delta t)$ is kept constant.

Pressuremeter test results in sandy soils

Typical values of the compressibility factor β fall in the range $[0.02; 0.12]$ for sandy soils [3]. Numerical computations of the dilatometer test were conducted assuming the values reported in Table I. Only the parameters that significantly affect the pressure–volume curve are indicated in Table I. The soil is considered as normally consolidated and fully saturated. Plane strain conditions (that enable to transform the pressure–volume curve into a pressure–strain curve) and fully drained conditions are also assumed. The axisymmetric geometry with a ratio of the outer diameter $2b$ to the inner diameter $2a$ equal to 50 follows the recommendations by Bahar [8] in the case of a sandy soil (Figure 4). In Figure 4, σ_{r0} represents the initial radial stress and $\sigma_r(a) = \sigma_{r0} + \Delta p$ the radial stress at the borehole wall (Δp is the pressure increment applied by the probe).

The finite element computations reveal that in that case, the compressibility factor β clearly affects the effective radial stress σ'_r–cavity strain δ_a curve where δ_a is the ratio of the cavity wall displacement to the initial radius a of the cavity (Figure 3). The results show that the plastic compressibility can be accurately identified by inverse analysis. A similar conclusion is obtained when the unloading of the horizontal stress due to the drilling phase is taken into account [1].

However, can the plastic compressibility be determined simultaneously with several other parameters of the Cam-Clay model?

Simultaneous determination of several key parameters

For that purpose, an inverse analysis of pressuremeter tests results was developed. The inverse analysis consists in minimizing the difference between experimental data and the outcome of analytical or, in the present case, numerical calculations. The fitting of experimental data with numerical computations is achieved by combining the direct modelling scheme and a parameter optimization routine. The method is illustrated in Figure 5. In this section,

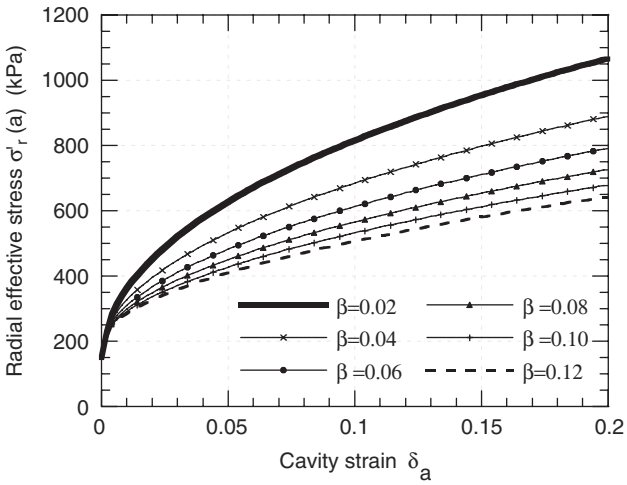

Figure 3. Effect of the compressibility factor β on the pressure–strain curve.

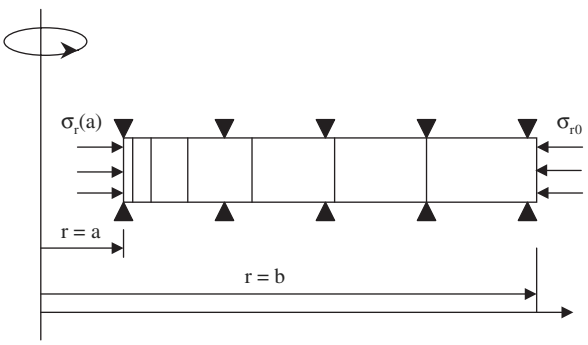

Figure 4. FEM model.

a pseudo-experimental set of data (subsequently named reference set of data) was constructed by a direct numerical computation assuming the parameter values in Table I and a compressibility factor β equal to 0.06.

As previously mentioned, the parameters of the modified Cam-Clay model have not the same effect on the pressure–volume curve. A sensitivity study showed that the key factors which significantly affect the results are the shear modulus G, the slope of the critical state line M, the plastic compressibility β, the effective pre-consolidation pressure p'_{c0} as well as the initial state of stress, the strain loading rate or the permeability of the sand formation and therefore the drainage conditions. The parameters (for example, the Poisson's ratio v) which have no effect on the pressure–volume curve cannot be optimized objectively and have therefore to be assumed, based on recommendations, standards or laboratory test results.

The determination of the first four parameters by inverse analysis was qualitatively investigated. A perturbation introduced in the value of one, two or three selected parameters

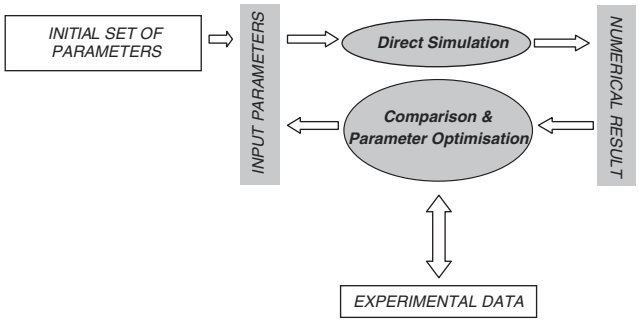

Figure 5. Flow chart of the inversion procedure.

Table II. Simultaneous identification of β, M and p'_{c0} from one curve in drained conditions.

Parameter	Unit	Reference	Initial value	Optimized value
β		0.06	0.03	0.035
M		1.2	1.00	0.92
p'_{c0}	kPa	280	400	335

generated an initial set of input data for the inversion process. The ability of the inverse method to converge towards the reference value was then examined.

The conclusions of this preliminary study are that the identification of a single parameter among G, M, β or p'_{c0} is feasible from a single pressure–strain curve obtained in drained conditions. When two parameters have to be simultaneously identified, the following conclusions can be drawn:

- the couples (G, M) or (G, p'_{c0}) can be determined from one curve obtained in undrained conditions [5] but this is no longer the case for the couple (M, p'_{c0});
- the couples (M, p'_{c0}), (β, M) or (β, p'_{c0}) can be determined from one curve in drained conditions since the pressure–strain curve is in this case the material response in effective stresses [9].

As indicated in Table II, the simultaneous identification of β, M and p'_{c0} from one pressure–strain curve obtained in fully drained conditions, whatever the initial set of parameters may be, leads to erroneous estimates, even if the numerical predictions fit perfectly the pseudo-experimental data (Figure 6).

Additional experimental information is therefore required to improve the optimization process. For instance, for clay, it is possible to enrich the experimental data by the measurement of the pore-water pressure $u(a)$ at the cavity wall [6]. In the present case, the experimental device does not allow to record the pore pressure. Therefore, the inverse procedure was carried out considering two pressure–strain curves obtained in different drainage conditions, one in fully drained conditions, another in fully undrained or partially undrained conditions. The results

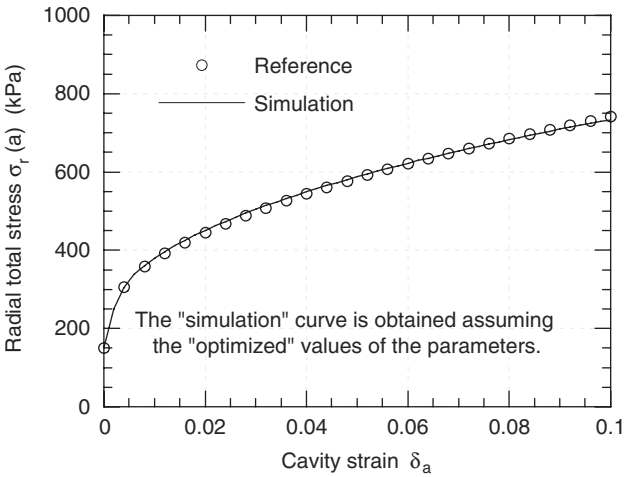

Figure 6. Comparison of experimental and optimized pressure–strain curves.

Table III. Simultaneous identification of β, M and p'_{c0} from two curves (fully drained and fully undrained conditions).

			Initial values		Optimized values	
Parameter	Unit	Reference	Calculation 1	Calculation 2	Calculation 1	Calculation 2
β		0.06	0.03	0.12	0.06	0.061
M		1.2	0.95	1.40	1.20	1.19
p'_{c0}	kPa	280	600	1500	279.9	280

presented in Table III for two initial sets of perturbed data showed the capability of the procedure for determining simultaneously the three parameters β, M and p'_{c0}.

Conclusions of the feasibility study

The previous numerical study shows that the effect of the compressibility factor β is important enough to allow an accurate determination from a pressure–strain curve obtained in drained conditions. From the various attempts, the simultaneous identification of up to two parameters can be achieved with satisfactory accuracy from one single pressure–strain curve. Finally, if two pressure–strain curves obtained for very different drainage conditions are considered in the inverse procedure, then the compressibility factor β, the slope of the critical state line M and the effective pre-consolidation pressure p'_{c0} can be simultaneously identified. As currently done, an experimental determination of the last key factor, namely the shear modulus G, can be obtained from an unloading–reloading cycle during the field test [10].

DEFINITION OF THE EXPERIMENTAL PROGRAM

In order to specify the experimental program, some additional computations were performed assuming more realistic *in situ* conditions than previously. A normally consolidated shallow weakly-to-non-cemented sand reservoir at a depth of several hundred metres was considered (confidentiality prevents us to be more precise about the depth of the tests). The new set of constitutive parameters and initial conditions is given in Table IV where p'_0, q_0 and u_0 are, respectively, the initial mean effective stress, the initial stress deviator and the initial pore pressure (the coefficient of earth pressure at rest is taken equal to 0.5). The formation permeability and the *in situ* oil viscosity yields to a value of k equal to 10^{-7} m/s for the permeability coefficient of the Darcy's law [1], assumed to be isotropic even if a certain amount of anisotropy should exist. It has been shown that the permeability anisotropy has no effect on the results of a pressuremeter test provided that the vertical permeability coefficient is lower than or equal to the horizontal permeability coefficient [7].

As previously indicated, the pore pressure generation is governed by the soil permeability and the initial strain rate of the test (Equation (1)). Considering the initial stress state and soil characteristics presented in Table IV, the undrained conditions are achieved for an initial strain rate greater than $2 \times 10^{-4}\,s^{-1}$ and the fully drained conditions for an initial strain rate lower than $2 \times 10^{-8}\,s^{-1}$, which corresponds to values of D_k, respectively, greater than 100 and lower than 0.01 or to stress rates, respectively, equal to 500 and 0.05 kPa/s.

The computations confirm the effect of the stress rate $(\Delta\sigma_r(a)/\Delta t)$ on the radial effective stress $\sigma'_r(a)$ and the pore pressure $u(a)$ at the cavity wall (Figure 7). Stress rates greater than 16.67 kPa/s (1000 kPa per minute) induce a complete development of the pore pressure. On the contrary, stress rates lower than 1.67 kPa/s (100 kPa per minute) involve the complete development of the radial effective stress and a limited pore pressure generation. The fully undrained conditions are unrealistic in practice since they require a very large value of the pressure rate. Therefore, one of the two pressure–strain curves necessary for the inverse procedure has to be obtained in partially undrained conditions, the second one corresponding to a fully drained condition.

Previous calculations were based on a well-defined value of the permeability coefficient. Although the permeability coefficient has a strong influence on the evolution of both the pore pressure and the radial effective stress, it cannot be integrated in the inverse procedure for identification without the knowledge of the pore pressure dissipation [6]. Since its value has to be assumed, a wrong estimate can therefore significantly change the results of the optimization process, mainly the optimized value of the compressibility factor β. Then, the effect of the permeability value on the optimized set (β, M, p'_{c0}) is now examined.

As in the previous section, two reference pressure–strain curves were numerically constructed, the first one in fully drained condition and the second one in partially undrained condition assuming a value of the permeability coefficient of 5×10^{-7} m/s. The modified Cam-Clay

Table IV. Modified Cam-Clay parameters for petroleum application.

Parameter	G	β	M	p'_{c0}	k	p'_0	q_0	u_0
Unit	MPa			kPa	m/s	kPa	kPa	kPa
Value	1130	0.06	1.16	5332	10^{-7}	3730	2800	6000

Note: k, coefficient of permeability; p'_0, initial mean effective stress; q_0, initial stress deviator; u_0, initial pore pressure.

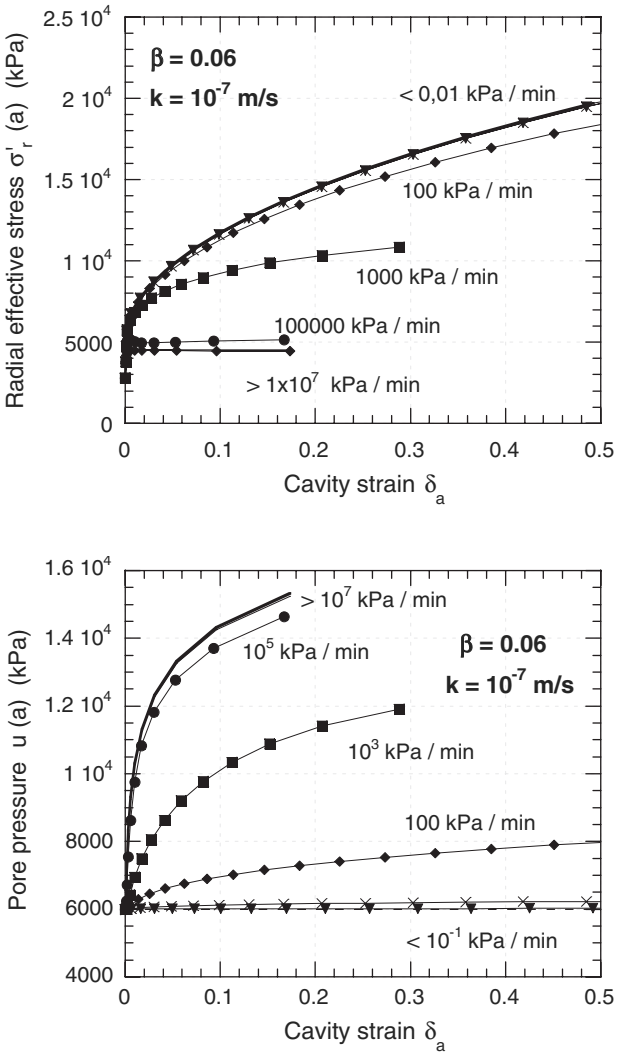

Figure 7. Effect of the stress rate on the effective radial stress and the pore pressure at the cavity wall.

parameters and the initial state of stress are given in Table IV. The value of the permeability coefficient was then changed and the optimization procedure was performed. The newly optimized values of β, M and p'_{c0} are of course different from the reference set of parameters. The gap is noted $\Delta\beta$, ΔM or $\Delta p'_{c0}$. The discrepancy, defined as the ratio between the gap and the reference value of the parameter, is represented in Figure 8 in the case of an equal numerical weight given to the two pressure–strain curves. The relative error increases greatly when the permeability coefficient is underestimated or overestimated by a factor 10.

Two possibilities were envisaged to decrease the potential errors. The first one was to enrich again the experimental data by adding a third pressure–strain curve carried out in different drainage conditions than the two first tests. No improvement was observed. The second one was

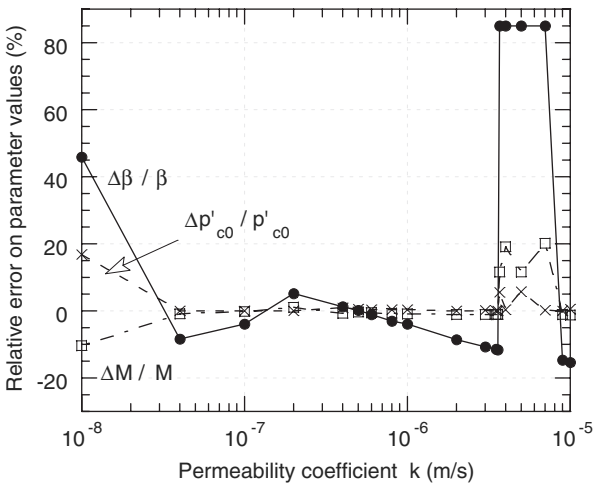

Figure 8. Effect of an erroneous estimate of k on the optimized parameters (equal weight).

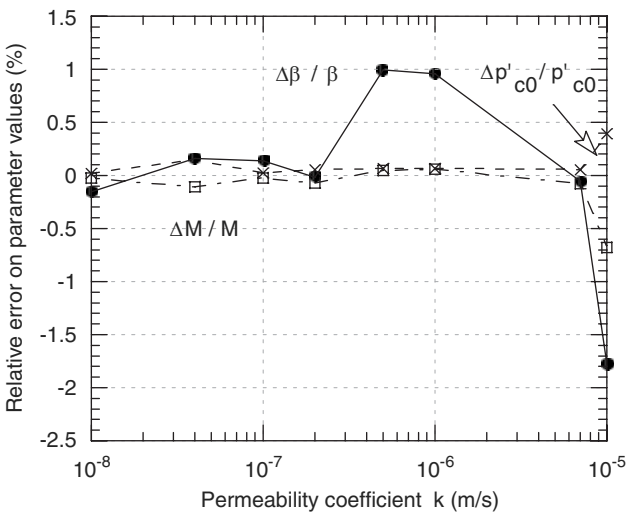

Figure 9. Effect of an erroneous estimate of k on the optimized parameters (different weights).

to numerically provide a more important weight to the test carried out in fully drained conditions in the optimization process. Indeed, the formulation of the inverse code contains the definition of a weighting matrix used for the estimation of the difference between the experimental data and the numerical simulations. Basically, the weighting matrix was introduced to take into account a more or less important uncertainty on the measured experimental data. A more important weight was given to the variables measured with a better accuracy [11]. That was the case for the test carried out in fully drained, since the curve represents directly the response of the soil skeleton in effective stresses. The weight of the second curve obtained in partially drained conditions was lowered since this curve was more dependent on the value of the permeability coefficient. As shown in Figure 9, this second option caused

a clear improvement of the optimization results since the error appeared to be lower than 2%, whereas the permeability coefficient was changed by a factor 100. This solution will be systematically used in the inverse procedure later on.

DILATOMETER TESTS

Based on the positive results of the above-mentioned numerical investigation, an experimental campaign was planned in a shallow weakly-to-non-cemented sand reservoir. The dilatometer (Figure 10) is a tool designed for measuring the radial displacement of the cavity of a borehole in response to a pressure increase [1]. It consists of an inflatable membrane fitted with three displacement sensors capable of measuring the radial displacements of the membrane and a pressure gauge providing the fluid pressure inside the membrane. The pressurization system

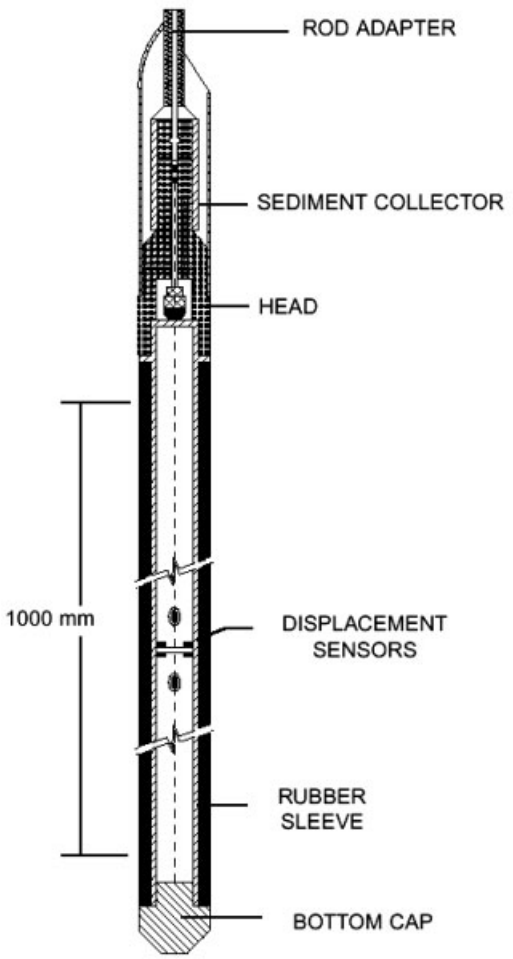

Figure 10. Schematic view of the dilatometer (after Marchina *et al.* [1]).

consists of standard compressed nitrogen cylinders. The height to diameter ratio of the dilatometers used in this study is greater than 10, justifying the plane strain condition hypothesis [12]. Mainly used to identify the elastic properties of a rock mass, the field of application of the dilatometer is specifically extended here to the characterization of both the elastic and plastic parameters of the oil sand reservoir.

A series of three dilatometer tests was conducted in an undepleted reservoir in which a pilot hole was carried out and both gamma ray and resistivity observations were done to accurately define the depths of the subsequent dilatometer tests. The operational sequence consisted of (i) the drilling of the well down to the top of the potential test interval, (ii) the coring of the test interval, so as to ensure maximum borehole wall quality and (iii) the performing of the test itself.

A dilatometer of 90 mm in diameter was slowly and carefully lowered in a newly drilled well for carrying out the first two tests. The diameter of the hole had to allow sufficient clearance between the tool and the borehole wall so that it was possible to run the tool, but that clearance had to be minimized so as to maximize the useful range of the displacement sensors. The coring tool, 98.425 mm in diameter, was specially designed for that operation. The test hole was vertically cored and logged with a caliper before lowering the dilatometer. It was found perfectly smooth.

The first test (Figure 11) consisted in increasing the pressure at a low stress rate (100 kPa per minute) until the maximum pressure or displacement (20 mm) was reached, depending on which would occur first. Three unloading–reloading stages were performed at the same rate to assess the elastic properties of the formation at different stress levels. The amplitude of the cycles was limited to the initial stress deviator in order to avoid any plasticity during the unloading stage. The second test, a few metres deeper, in the same sand unit, was similar to the first one, but unloading–reloading cycles were conducted at a much higher rate (1000 kPa per minute). The dilatometer was damaged during the pulling out after the second test (associated with a malfunction of the data acquisition system giving a spiky readout) and was replaced by a dilatometer of 95 mm in diameter for the third test conducted in a deeper sand unit following the same loading program than the second test. The third test showed an unusual shape not conforming to the expectations and was considered as not significant.

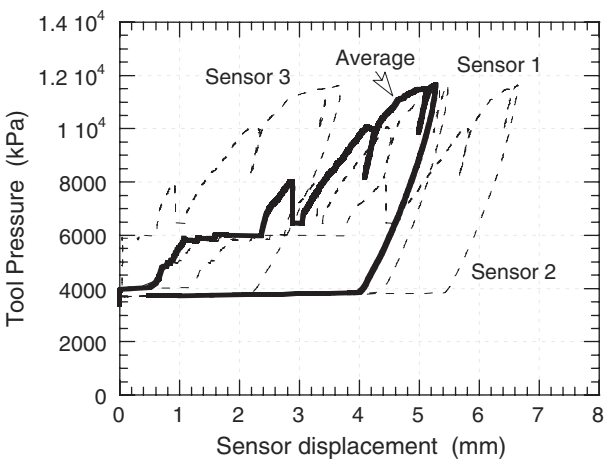

Figure 11. Raw data of the first dilatometer test.

As a consequence, only the raw experimental data corresponding to the first test are presented in Figure 11. Dotted lines represent the readings given by each of the three displacement sensors, whereas the continuous line represents the average curve. Although the curves have globally the same features for the three sensors, the amplitudes do not match exactly. This is most likely due to a slight asymmetry of the borehole or some degree of horizontal anisotropy in the tested formation. The initial part of the curves shows that the initial displacements are measured without noticeable pressure change, which indicates a free inflation of the membrane due to a lack of contact between the membrane and the borehole wall. As soon as the tool comes to contact with the borehole wall, the curve steepens up.

ANALYSIS OF THE EXPERIMENTAL DATA

This first experimental attempt encountered technical difficulties inherent in the extreme conditions of the testing. Only the first test is reasonably exploitable for the purpose of parameters identification. The inverse procedure described previously, which requires at least two tests carried out at different stress rates, cannot be consequently performed. However, it was demonstrated that the couple of parameters (β, p'_{c0}) could be determined from a single pressure–displacement curve in fully drained conditions, provided that the values of the shear modulus G and the critical state parameter M are either measured in another way or assumed.

The raw data of the first test were carefully examined and pre-processed in order to keep the significant part of the pressure–displacement curve, discarding the initial part until the contact between the tool and the borehole was firmly established (Figure 12). The cavity strain δ_a was calculated by dividing the average displacement of the borehole by its initial radius. The unloading–reloading stage was not considered in the inverse procedure, except for the measurement of the shear modulus G as follows:

$$G = \frac{E}{2 \times (1 + \nu)} = \frac{\Delta\sigma_r(a)}{2\Delta\delta_a} \tag{2}$$

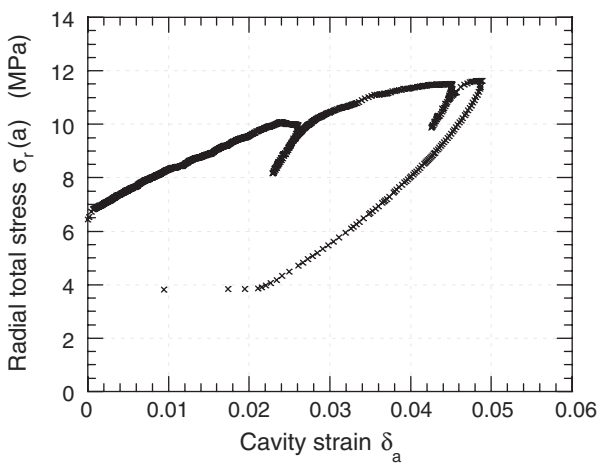

Figure 12. Pre-processed data for inverse analysis of the first test.

where E is the elastic modulus, $\Delta\sigma_r(a)$ and $\Delta\delta_a$ are, respectively, the variations of the radial stress and the circumferential strain at the cavity wall in the unloading–reloading cycles. The value of the shear modulus in the different cycles was between 230 and 270 MPa, which corresponds to a value of the elastic modulus E between 600 and 700 MPa assuming a Poisson's ratio of 0.3. Although the results are fairly consistent from one cycle to the other, the values found are unexpectedly small, considering the depth of the tested soil. Likewise, the initial slope of the pressure–strain curve gives a pseudo-shear modulus of 81 MPa, that is to say an elastic modulus of 210 MPa.

A series of direct simulations of the first test was performed with the goal to define an acceptable range of variation for the parameters related to the compressibility of the sand reservoir. In those computations, the following values were assumed: the critical state parameter M was taken equal to 1.16, the compressibility factor β to 0.09, the Poisson's ratio to 0.3 and the initial void ratio e_0 to 0.43. The value of the initial state of stress and the pre-consolidation pressure were deduced from the experiments, assuming a normally consolidated behaviour. The test was also supposed to be perfectly drained.

None of the values was assumed for the elastic modulus E but the value deduced from the initial slope of the pressure–strain curve enabled to even coarsely fit the initial part of the curve (Figure 13). Therefore, the elastic modulus E was set to 210 MPa. A similar sensitivity study than in the case of the permeability coefficient was performed to assess the error made on the optimized parameters if the value of the elastic modulus was under-estimated or over-estimated. Figure 14 indicates that potential errors on the couple (β, p'_{c0}) can occur if the elastic modulus is under-estimated or over-estimated. A similar conclusion is obtained if the critical state parameter M is under-estimated or over-estimated (Figure 15).

Nevertheless, large variations of the critical state parameter M, of the elastic modulus E and even of the compressibility factor β do not allow to correctly fit the computations to the experimental data. Therefore, one of the initial assumptions had to be reconsidered. The value of the pre-consolidation p'_{c0} was changed such as the over-consolidation ratio R varied

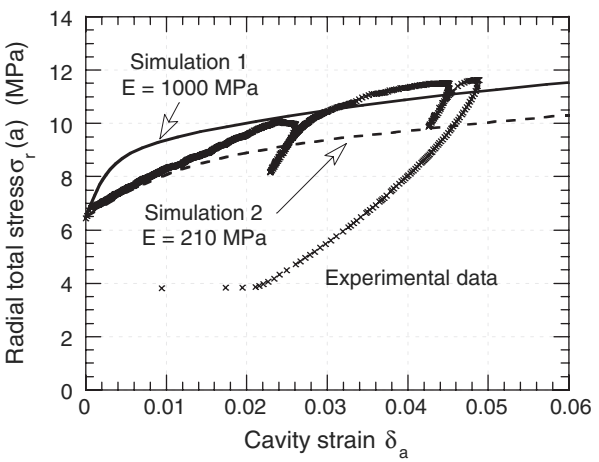

Figure 13. Fitting of the elastic modulus E.

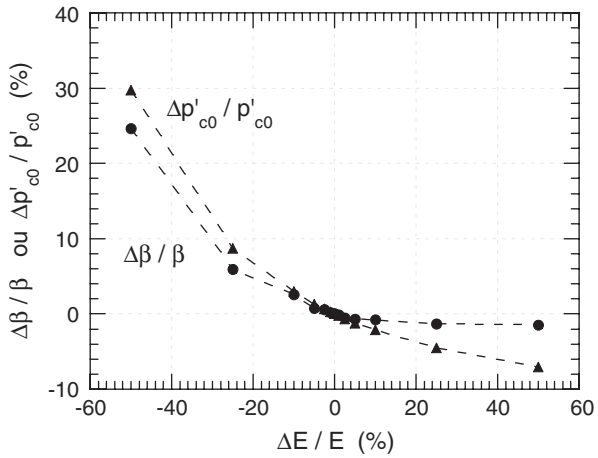

Figure 14. Potential error on the optimized parameters as a function of an error on E.

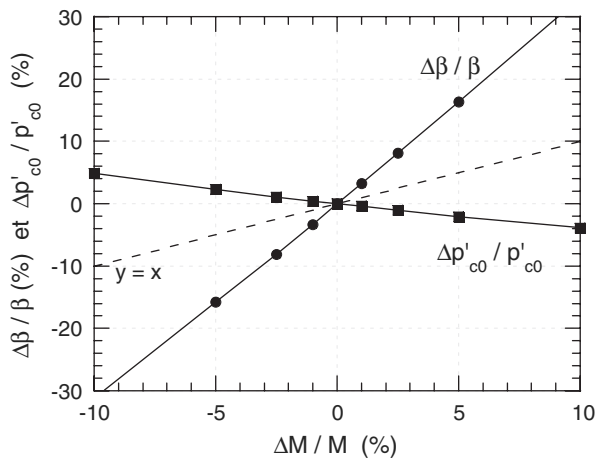

Figure 15. Potential error on the optimized parameters as a function of an error on M.

between 1 and 2 in order to simulate an over-consolidated behaviour for the tested formation (Figure 16). The over-consolidation ratio R is defined as the ratio between the pre-consolidation pressure p'_{c0} (intercept of the hydrostatic axis and the yield surface in the p'–q diagram) and the initial mean effective stress p'_0 [13]. Figure 16 shows that an over-consolidation ratio R close to 1.7 allows to match the experimental data and the computational results. Unfortunately, at such a level of over-consolidation, it appears that the compressibility factor β no longer impacts the response of the dilatometer simulation, which means that in such a specific case, the value of the plastic compressibility cannot be accurately identified.

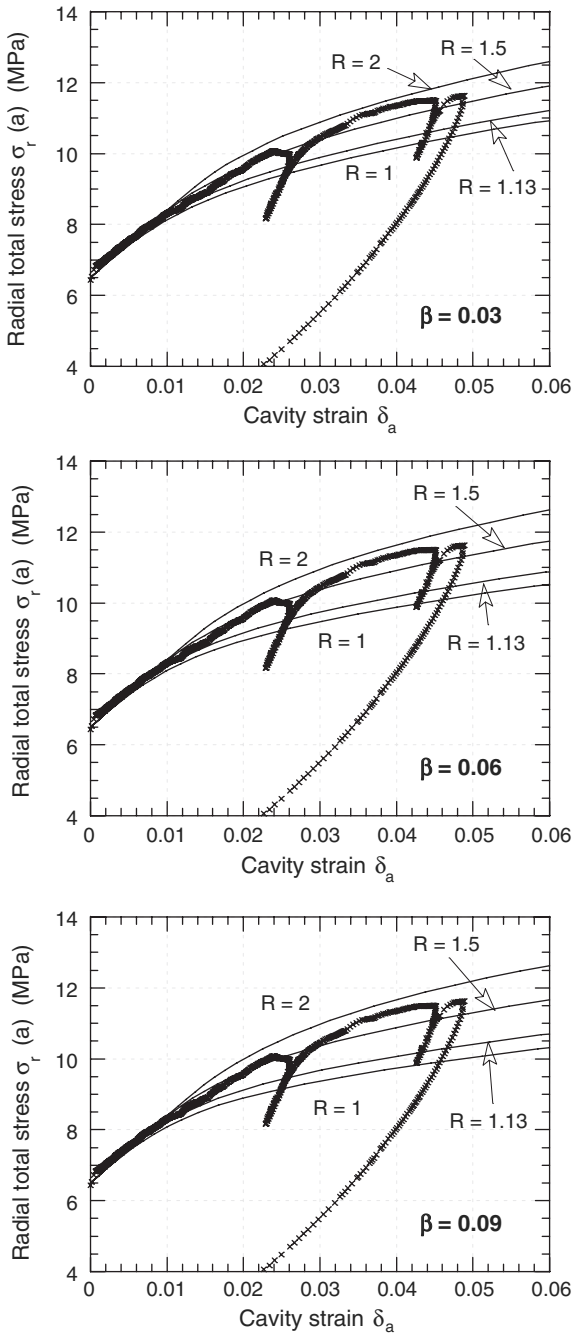

Figure 16. Effect of the over-consolidation ratio R on the simulations.

COMMENTS

The previous conclusion can be interpreted in several ways. The existence of a cohesion due to a light cementation could produce a behaviour such as recorded. Another explanation could be that a significant erosion of the site took place [1], in which case it would imply that, at some stage in its history, the reservoir was buried at a greater depth than the current one. Geologists and the analysis of logs in several wells of the same oil field have subsequently supported that last observation as the more likely cause for the observed strong over-consolidation. Since the formation is over-consolidated, the compaction caused by the decrease in the pore pressure during production will take place in the elastic domain until a state of stress is reached that corresponds to the current consolidation pressure. Beyond that point, after a significant amount of depletion, plastic compaction will occur at a larger rate of deformation than in the elastic domain, leading to an increased compaction of the sand formation.

The relevance of the chosen constitutive model has also to be questioned. First, the process implies a certain amount of unloading before inserting the probe in the borehole. That phase was found to have only a minor effect on the initial part of the subsequent loading stress–strain curves considering the model adopted here [14, 15]. More, during the first test, some viscous effects were pointed out: an important creep of the soil was noticed while the pressure was kept constant for a few minutes. A time-dependent behaviour was also observed during the unloading–reloading stages carried out at the same pressure rate than the loading phase. Further work will consist in implementing a visco-elasto-plastic model into the finite element code and in adapting the operational procedure. Improvements could also be brought to the model in order to consider specificities such as the anisotropic fabric of the subsoil or the heterogeneity at the cavity wall. Indeed, a thick compressible filter cake at the borehole wall could affect the pressure–displacement curve. Additional numerical computations considering a thickness of the cake equal to 10% of the initial radius of the borehole showed that the effect of the elastic modulus E and the compressibility factor β of the cake can influence the results for values, respectively, lower than 50 MPa and greater than 0.2. Nevertheless, the main conclusion was that a thick compressible filter cake has only a limited effect on the results of a dilatometer test.

CONCLUSIONS

Based on previous analysis on pressuremeter tests in clays, this study showed that, under some conditions, the plastic compressibility of an oil sand formation could be accurately identified by inverse analysis of dilatometer tests. This work also aimed at defining the best operational procedure in order to simultaneously determine the plastic compressibility β, the pre-consolidation pressure p'_{c0} and the slope of the critical state line M in the $(p–q)$ diagram of the modified Cam-Clay model. The comparison between experimental data and direct numerical simulations revealed that the assumption of a normally consolidated subsoil was not suitable in the present case. All the data subsequently collected in the site led to the conclusion that an over-consolidation ratio R close to 1.7 should represent the initial state of the sand formation. It was therefore not possible to accurately identify the value of the plastic compressibility. However, *in situ* measurements of oil sand compressibility

by means of dilatometer tests was theoretically recognized as an interesting approach to evaluate the importance of the compaction drive for the production of an oil field.

ACKNOWLEDGEMENTS

The authors express sincere appreciation to Total E&P for their confidence and the permission to publish the results. They also would like to acknowledge Me2i for the carrying out of the *in situ* dilatometer tests.

REFERENCES

1. Marchina P, Brousse A, Fontaine J, Dano C, Alonso C. In situ measurement of rock compressibility in a heavy oil reservoir. *International Thermal Operations and Heavy Oil Symposium Itohos*, *Paper SPE 86940*, Bakersfield U.S.A., 2004.
2. Roscoe KH, Burland JB. On the generalised stress–strain behaviour of 'wet clay'. *Engineering Plasticity*. Cambridge University Press: Cambridge, 1968; 535–609.
3. Biarez J, Hicher P-Y. *Elementary Mechanics of Soil Behaviour—Saturated and Remoulded Soils*. Balkema: Rotterdam, 1994.
4. Colliat-Dangus J-L. Comportement des matériaux granulaires sous fortes contraintes—influence de la nature minéralogique du matériau étudié. Thèse de doctorat-sciences, Université de Grenoble, 1986.
5. Zentar R, Hicher P-Y, Moulin G. Identification of soil parameters by inverse analysis. *Computers and Geotechnics* 2001; **28**(2):129–144.
6. Rangeard D, Hicher P-Y, Zentar R. Determining soil permeability from pressuremeter tests. *International Journal of Numerical and Analytical Methods in Geomechanics* 2003; **27**(1):1–24.
7. Rangeard D, Zentar R, Hicher P-Y, Moulin G. Permeability effect on pressuremeter test results. *8th International Symposium on Numerical Methods in Geomechanics NUMOG VIII*, Rome (Italy), 2002; 619–625.
8. Bahar R. Analyse numérique de l'essai pressiométrique: application à l'identification de paramètres de comportement des sols. *Ph.D. Thesis*, Ecole Centrale Lyon, 1992 (in French).
9. Rangeard D, Dano C, Marchina P. Identifying soil compressibility from pressuremeter test. *9th International Symposium on Numerical Models in Geomechanics NUMOG IX* Ottawa (Canada), 2004; 683–689.
10. Bolton MD, Whittle RW. A non linear elastic perfectly plastic analysis for plane strain undrained expansion tests. *Geotechnique* 1999; **49**(1):133–141.
11. Ecole Nationale Supérieure des Mines de Paris. *SiDoLo Version 2.3*. *User Manual*, Ecole Nationale Supérieure des Mines de Paris, 1995.
12. Houlsby GT, Carter JP. The effect of pressuremeter geometry on the results of tests in clay. *Geotechnique* 1993; **43**(3):567–576.
13. Wroth CP. The interpretation of in situ soil tests. *Geotechnique* 1984; **34**(4):449–489.
14. TotalFinaElf. Mesure in-situ de la compressibilité des roches. Internal document.
15. Cambou B, Bahar R. Utilisation de l'essai pressiométrique pour l'identification de paramètres intrinsèques du comportement d'un sol. *Revue Française de Géotechnique* 1993; **63**:39–50.